Effects of ceramic processing parameters on the microstructure and dielectric properties of $(Ba_{1-x}Ca_x)(Ti_{0.99-y}, Zr_yMn_{0.01})O_3$ sintered in a reducing atmosphere

WEN-HSI LEE
Ceramic Material Development Department, Philips Passive Components Kaohsiung, Taiwan
TSEUNG-YUEN TSENG
Department of Electronic Engineering, National Chiao-Tung University, Hsinchu, Taiwan
D. HENNINGS
Philips Research Laboratory Aachen, 5100 Aachen, Federal Republic of Germany

The effect of A/B ratio, sintering temperature, and oxygen partial pressure on microstructure and ceramic dielectric properties of 1 mol % MnO_2 doped (Ba,Ca)(Ti,Zr,)O_3 sintered in a reducing atmosphere were investigated. Microstructure is found to be closely related to processing parameters. With decreasing A/B ratio, decreasing oxygen partial pressure and increasing sintering temperature, grain growth is enhanced. Concurrent with the grain size reduction, the crystal structure transformed from tetragonal to pseudocubic at room temperature and the dielectric constant, the dissipation factor and Curie point all decreased. However, the effects of grain size give a marked discrepancy on breakdown. The effect of A/B ratio and sintering temperature both suggest that breakdown voltage is decreased with increasing grain size. However, the breakdown voltage in relation to grain size by changing the oxygen partial pressure seems to show no significant difference.

1. Introduction

Dielectric ceramic formulation and process technologies for multilayer ceramic capacitors have been extensively investigated in the electronics industry [1]; recently multilayer capacitors with base-metal internal electrodes such as nickel have been developed to reduce the process cost [2], wherein, the dielectric should be co-fired in a reducing atmosphere to prevent the oxidation of the internal electrode. However, $BaTiO_3$ ceramics become semiconducting and lose their high insulation resistance due to the unlocalized electrons produced by the formation of oxygen vacancies due to the sintering in a reduced oxygen partial pressure [3]. To overcome this problem, Mn is often added to maintain high insulation resistance even after sintering in a reducing atmosphere, by trapping electrons to form a lower oxidation state. Dielectric properties and microstructure of $BaTiO_3$-based dielectrics are sensitively dependent on various factors such as the amount of additive and nature of sintering atmosphere, sintering temperature and stoichiometry of the composition [4, 5]. It is well known that processing parameters often show a dramatic influence on microstructure and dielectric properties of donor-doped $BaTiO_3$. However, the effect of processing parameters on microstructure and dielectric properties of acceptor-doped $BaTiO_3$ when sintered in a reducing atmosphere is not yet completely understood; in addition, the influence of microstructure on dielectric properties of MnO_2-doped BCTZ sintered in a wet reducing hydrogen atmosphere of H_2/H_2O is still not understood.

In the present work, the influence of *A/B* ratio and processing parameters such as sintering temperature and atmosphere on the dielectric properties of (Ba,Ca)(Ti,ZrMn)O_3 has been examined. Also, the grain size dependence of the crystallographic structure and dielectric properties are investigated in this study.

2. Experiments

2.1. Sample preparation

The samples were prepared from high purity $BaTiO_3$ (Nippon-Chemical), TiO_2 (Fuji Titanium), $CaCO_3$ (Merck), ZrO_2 (Merck) and MnO_2 (Merck) raw materials by using the conventional solid-state reaction method. The raw materials were weighed according to the chemical formula $(Ba_{1-x}Ca_x)_z(Ti_{0.99-y}, Zr_yMn_{0.01})O_3$ with x fixed at 0.13, y ranging from 0.140 to 0.132 in steps of 0.002 and z ranging from 0.993 to 0.999 in steps of 0.002. The cation ratio of A-site ion (Ba,Ca) and B-site ions (Ti,Zr,Mn) was carefully controlled and checked by

using X-ray fluorescence. Samples with A/B ratios of 0.993, 0.995, 0.997 and 0.999, were prepared.

All batches were wet ball-milled in a polypropylene bottle, dried and calcined at a temperature of 1000 °C for 4 h in an alumina crucible. Milling of calcined powders to an average particle size of 1 μm was carried out. These powders were pressed into disks with a diameter of 10 mm. Monolithic capacitors were prepared by the following method. To make slip, the calcinated powder was mixed with PVA binder, dispersant, defoamer agent and water. The resultant slurry was formed into 25 μm thick sheets. A paste to form the internal electrode containing nickel powder was screened onto the green sheet. These printed sheets were stacked, pressed, and cut to form monolithic capacitors.

Ceramic disks and monolithic capacitors were then sintered at different temperatures for 4 h in a series of variable moisture reducing atmospheres which were controlled by the equilibrium of H_2 and H_2O. Subsequently, annealing in an oxygen partial pressure below 1.7×10^{-6} Pa at 1000 °C was carried out to reoxidize the ceramic bodies. The annealed samples were polished and electroded with Dupont 7095 silver paste.

2.2. Microstructure observations

The examined surfaces of the sintered samples were lapped, ground and polished with 1 μm Al_2O_3 powder to a mirror-like finish and then chemically etched to reveal the grains. Carbon or gold deposition was applied on the surface of the samples to improve the resolution of the image. The surface microstructure was examined by scanning electron microscopy (SEM; Hitachi Model S5200). The average grain size was determined by the linear intercept method.

The formation of monophase BCTZM in the calcined powder and sintered samples were analyzed by using a Siemens D5000 X-ray diffractometer (XRD) with CuKα radiation and a Ni filter, operated at 20 KV and 40 mA. The operating parameters of the XRD included a scanning speed of 0.0067° per second and scanning from range 20° to 80°.

3.3. Electrical measurement

Using an automatic capacitance bridge (HP4278A), capacitance and dissipation factor of the samples were measured at 1 kHz/0.5 V_{rms} and the temperature dependence of the relative capacitance was studied in the range −50 °C to 150 °C. Insulation resistance was measured with HP 4140A after applying 50 V d.c. for 2 min and the breakdown voltage was measured at a rate of 100 V min^{-1} (detector current: 1 mA).

3. Results and discussion

3.1. Microstructure analysis

3.1.1. Effect of sintering temperature

Fig. 1A to D show the microstructures of BCTZM with A/B ratios of 0.993 sintered at 1260 °C, 1300 °C, 1340 °C and 1380 °C, respectively in a (3%/97%) H_2/N_2 reducing atmosphere. As expected, grain size is apparently increased with increasing sintering temperature. Fig. 2 shows the progression of microstructure development as a function of sintering temperature from 1260 to 1380 °C with 20 °C step for 2 h soaking time. The sintering process depends on the attainment of a lower energy state by a reduction in internal surface area. The surface always has a higher energy than the interior of a particle. Thus larger particles grow at the expense of smaller ones [6], densification is invariably accompanied by grain growth. The rate of densification is increased with the rate of transfer of material, with a corresponding increase in the rate of diffusion is ions. The presence of vacant sites and other defects assists diffusion. The concentration of vacant sites increases with temperature while other defects tend to disappear, consequently sintering occurs more readily at higher temperatures [7].

3.1.2. Effect of oxygen partial pressure

Fig. 3a to D show the microstructure of BCTZM with a A/B ratio 0.993 sintered at 1340 °C in 0.3%H_2, 1%H_2, 3%H_2 and 5%H_2 respectively. As the oxygen partial pressure increased from 3.25×10^{-14} to 7.82×10^{-12}, the grain size development was severely retarded. In agreement with previous study [11, 12], when $BaTiO_3$ is fired under reducing conditions, oxygen is lost from the lattice with the formation of doubly ionized oxygen vacancies and electrons in the conduction band.

Fig. 4 shows the progress of microstructure development as a function oxygen partial pressure at 1340 °C for 2 h soaking time. Apparently, grain size is increased with decreasing oxygen partial pressure. The affect of sintering under low oxygen pressure is to increase the concentration of oxygen vacancies, that is presumably to assist the diffusion of oxygen ions and enhance densification. Densification must be accompanied by the transfer of material and the rate at which it occurs depends on the rate of diffusion of ions. The presence of vacant sites and other defects assists diffusion [13].

3.1.3. Effect of A/B ratio

Fig. 5A to D show the microstructures of BCTZM with A/B ratios of 0.999, 0.997, 0.995 and 0.993, respectively, sintered at 1340 °C in a (3%/97%) H_2/N_2 reducing atmosphere. Apparently, small variations in non-stoichiometry of the order of 0.002 have resulted in significant changes in the grain growth behavior in BCTZM sintered in a reducing atmosphere. The average grain size of BCTZM, continuously decreases from 8.06 μm to 4.88 μm, with increasing A/B ratios from 0.993 to 0.999, as shown in Fig. 6.

Sintering temperature can be effectively reduced by including constituents that give rise to a liquid phase well below the melting point of the main phase. It is well known [8] that a small excess of TiO_2 reacts with $BaTiO_3$ to produce $Ba_6Ti_{17}O_{40}$ which forms along with $BaTiO_3$ a eutectic melt at 1320 °C. Therefore many authors [9, 10], noted that liquid phase sintering occurred at temperatures above the eutectic, the rapid grain growth is due to the existence of a liquid phase which improves the wettability of particles.

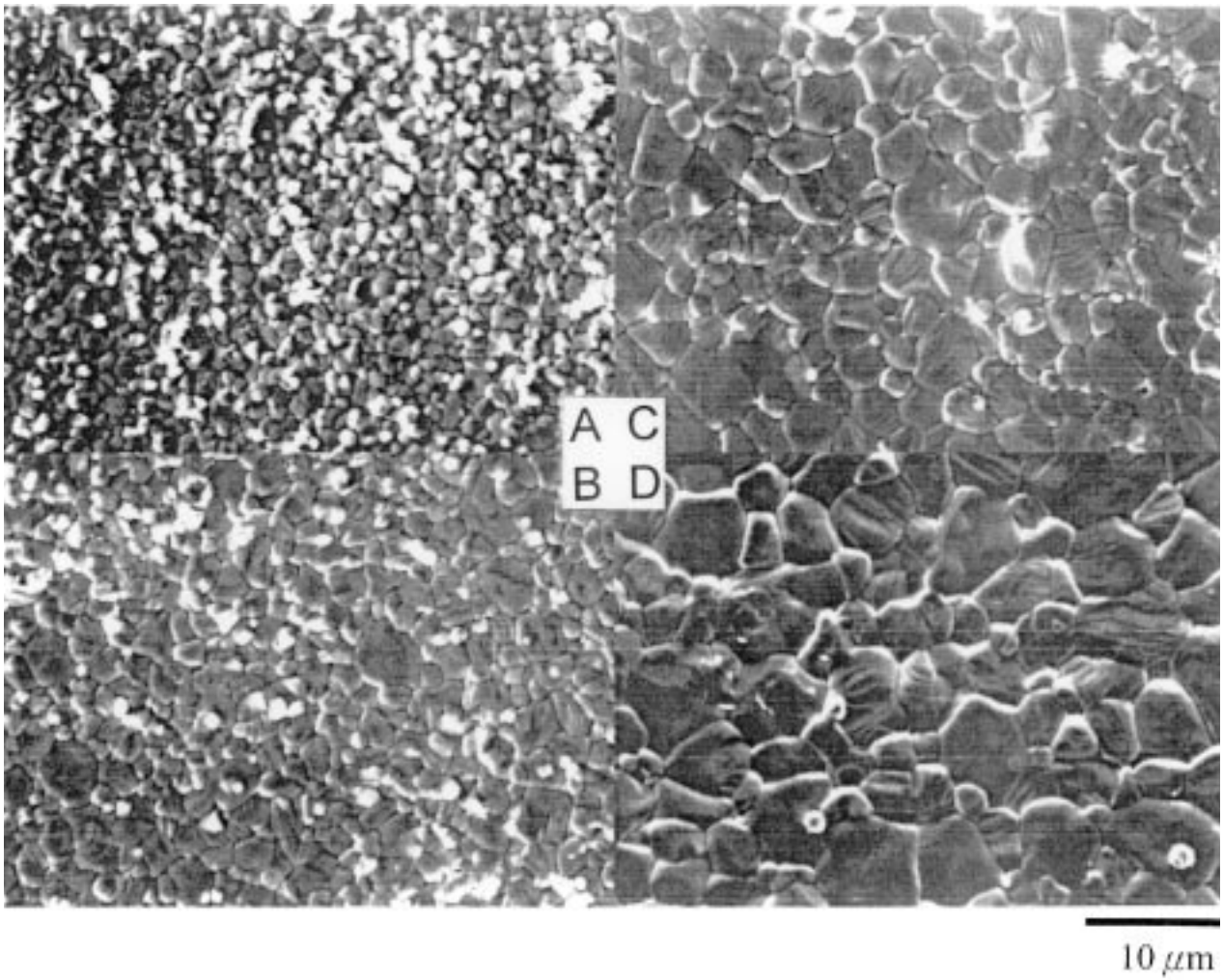

Figure 1 Scanning electron micrographs for samples of BCTZM with Ba/Ti = 0.993 sintered at (a) 1260 °C, (b) 1300 °C, (c) 1340 °C and (d) 1380 °C in 3% H_2/N_2 atmosphere and 25 °C H_2O.

3.2. Dielectric properties

3.2.1. Curie temperature, dielectric constant and dielectric loss

The microstructure plays an important role in determining the dielectric properties of the material. As stated previously, the grain size was significantly affected by A/B ratio, sintering temperature and atmosphere [14, 15]. The relationships between dielectric constant, dissipation factor and grain size are illustrated in Figs 7 and 8 which clearly indicate that dielectric constant and dissipation factor are both approximately proportional to grain size independent of the ceramic processing on modified grain size [16, 17]. Fig. 9 shows the dependence of Curie temperature on grain size which was influenced by A/B ratio, sintering temperature and sintering atmosphere. Similarly, Curie temperature is approximately proportional to grain size as well. This influence of grain size on Curie temperature is easily associated with the results of dielectric loss measured at 25 °C as a function of grain size. With decreasing grain size, the Curie temperature reduces, which corresponds to a reduction of the dielectric loss measured at 25 °C. On the other hand, the change of Curie temperature and dielectric constant with grain size is still not yet fully understood. The effect of grain size for these BCTZM samples with various A/B ratios sintered at 1340 °C in a 3% N_2H_2 reducing atmosphere on their dielectric properties, such as dielectric constant, loss tangent, breakdown voltage and Curie temperature are summarized in Table I. The dielectric constant is the maximal value at the Curie point, the loss tangent is measured at 25 °C and the breakdown voltage is measured at a rate of 100 V min^{-1}. We attempt to interpret this phenomenon by X-ray diffraction studies on BCTZM with different grain size due to change of A/B ratio.

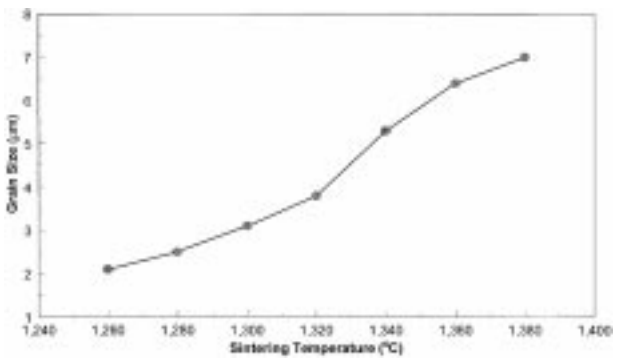

Figure 2 Relationship between mean grain size and sintering temperature for BCTZM samples.

Figs 10 and 11 show the dependence of dielectric

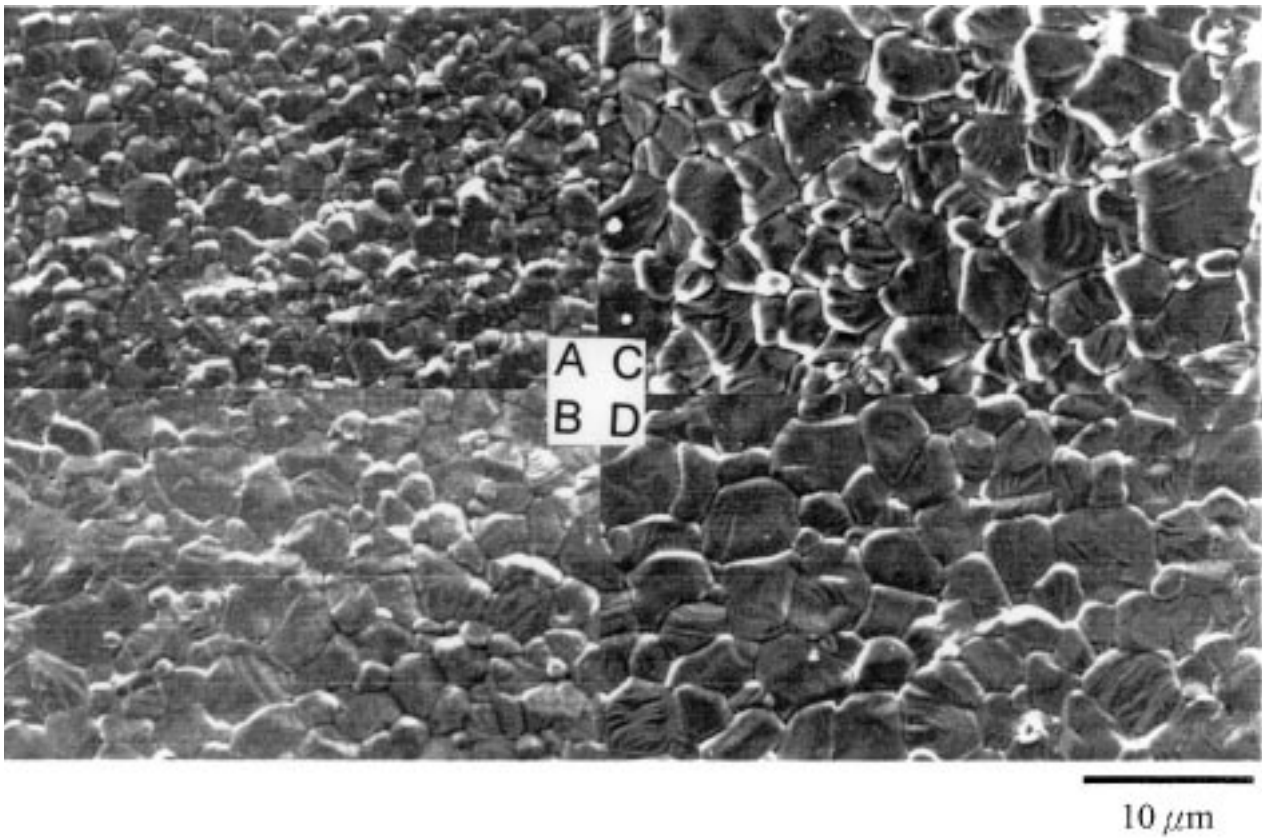

Figure 3 Scanning electron micrographs for samples of BCTZM with Ba/Ti = 0.993 sintered at 1340 °C in (a) 0.3% H_2/N_2 (b) 1% H_2/N_2 (c) 3% H_2/N_2 and (d) 5% H_2/N_2 atmosphere and 25 °C H_2O.

constant and dissipation factor of BCTZM, with various A/B ratios, on temperature, which depicts a strong temperature dependence with a maximum at the tetragonal-cubic transition. The reduction in grain size caused by increasing A/B was accompanied by a depression of the peak in permittivity at the Curie temperature and a general broadening of the phase transition. The diffuse phase transitions observed near the Curie point of the samples are attributed to the coexistence of ferroelectric and paraelectric phases [18]. When the material changes from the cubic paraelectric into the tetragonal ferroelectric phase, the internal stress in the microstructure increases strongly. A large portion of the resulting stress is compensated by ferroelectric domains, but the smaller the grain size becomes, the more incomplete the equalization of stress. The grain size thus has an immense influence on the temperature characteristics of these materials, as shown in Fig. 10. By reducing the average grain size of the ceramic BCTZM from 8.06 μm to 4.88 μm, the Curie maximum decreases from $K \approx 16\,000$ to $K \approx 11\,000$, and the Curie temperature is shifted from 23 °C to 8 °C when the A/B ratio is increased from 0.993 to 0.999. The Curie temperature is closely related to the A/B ratio and is believed to be mainly associated with the change of distribution of the tetragonal phase (ferroelectric state) and the cubic phase (paraelectric state).

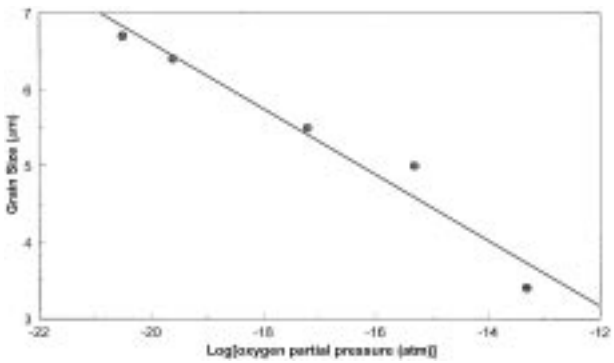

Figure 4 Relationship between mean grain size and oxygen partial pressure for BCTZM samples.

Fig. 12 shows, XRD patterns of BCTZ + 1 mol % MnO_2 with various A/B ratios. The X-ray patterns for BCTZM with various A/B ratios are almost identical. The group of lines (2 0 1) was chosen since it is more sensitive to the crystal structure changes. Lattice parameters ''*a*'' and ''*c*'' were calculated by employing a least squares fitting method. The *c*/*a* ratio for composition with different A/B ratio is shown in Fig. 13. It is observed that as A/B ratio is increased the *c*/*a* ratio continuously decreased close to unity at A/B ratio = 0.999 at room temperature. Fig. 12 shows the coalescence of the (2 0 1) and (1 0 2) doublets in one broad line, the changes of grain size accompanied by a decrease in the *c*-lattice parameter, in contrast to the slight increase in the *a*-lattice parameter, and a corresponding decrease in the *c*/*a* ratio, indicative of pseudocubic phase development. Thus, increasing the A/B ratio in the BCTZM lattice causes a transformation in the crystal structure from tetragonal to cubic at room temperature [19]. The proportions of ferroelectric and paraelectric phases are changed with different A/B ratios

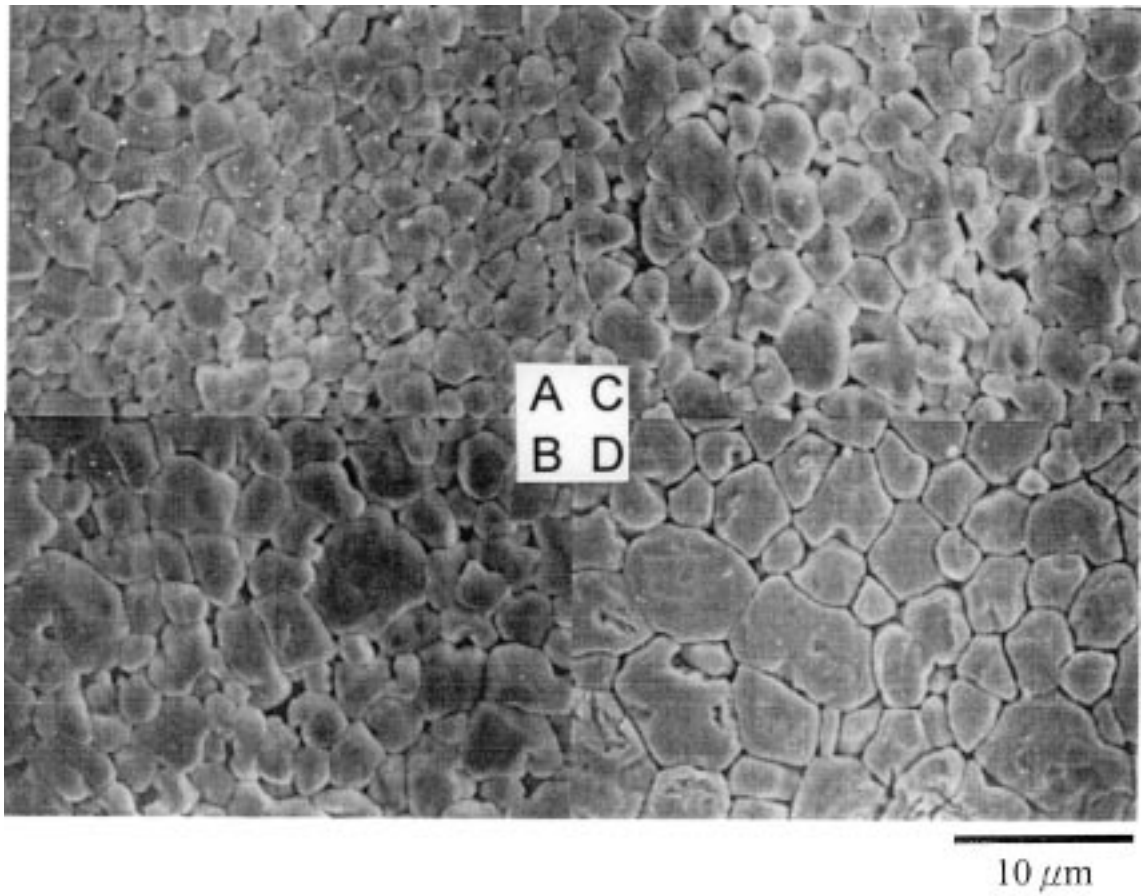

Figure 5 Scanning electron micrographs for BCTZM samples with (a) Ba/Ti = 0.999, (b) Ba/Ti = 0.997, (c) Ba/Ti = 0.995 and (d) Ba/Ti = 0.993 sintered at 1340 °C in 3% H_2/N_2 atmosphere and 25 °C H_2O.

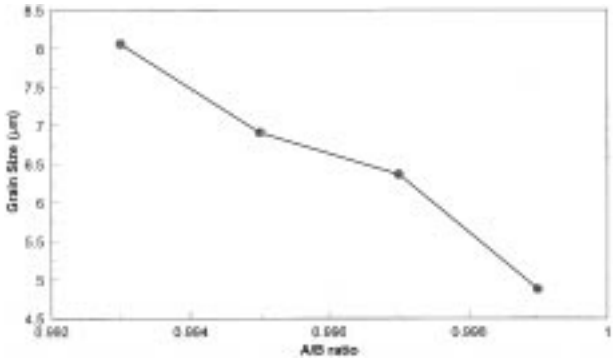

Figure 6 Relationship between mean grain size and A/B ratio for BCTZM samples.

from XRD measurements and contribute to the change of Curie temperature and the curve of the temperature dependence of capacitance. As mentioned previously, the tetragonality (c/a ratio) in higher A/B-ratio samples had essentially disappeared in favor of a pseudocubic structure formation, and the shift of Curie temperature (T_c) to lower temperture. The effect of stoichiometry on cell parameter and axial ratios of BCTZM samples is consistent with the grain size dominance of the structural characteristics described above. With the same particle size, sintered samples with small A/B ratio, in general, exhibit a lower Curie temperature than samples with large A/B ratios. This is presumably caused by the internal residual stresses generated during the sintering

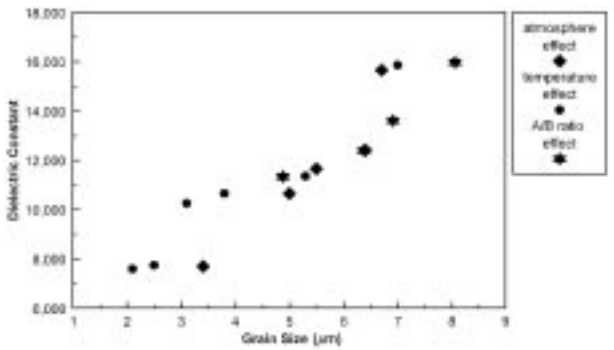

Figure 7 Dielectric constant as a function of mean grain size for BCTZM samples.

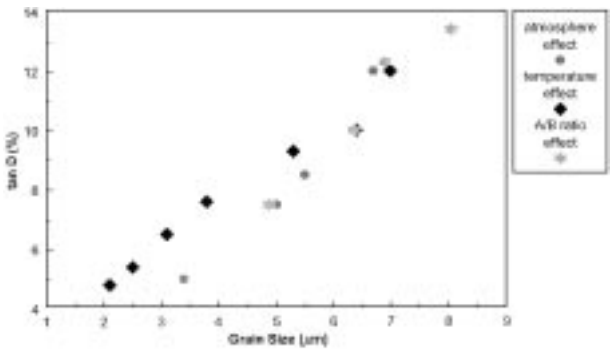

Figure 8 Loss tangent as a function of mean grain size for BCTZM samples.

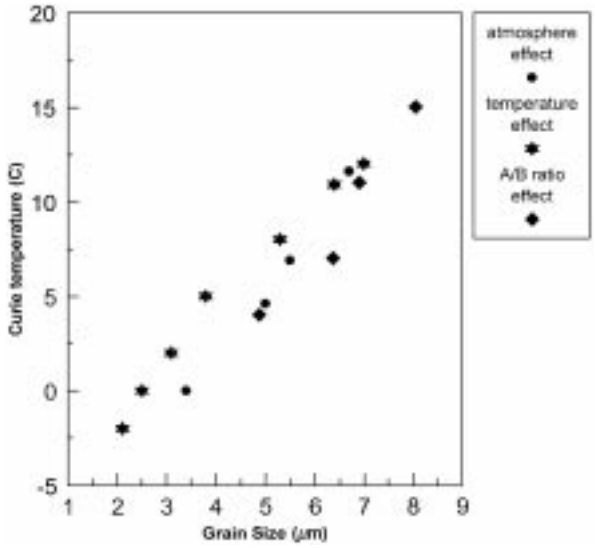

Figure 9 Curie temperature as a function of A/B ratio for BCTZM samples.

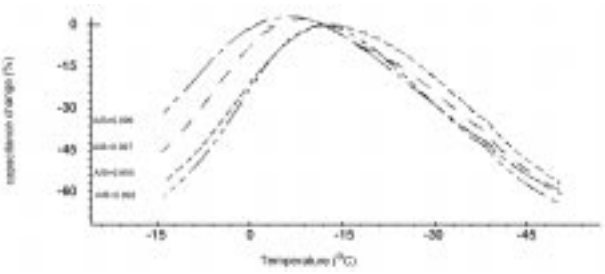

Figure 10 Temperature dependence of dielectric constant for BCTZM samples with various A/B ratios.

process [20]. The residual stress seems to be dependent on the grain size and is remarkable for small grain size. Therefore the drastic change in T_c is mainly attributed to the intrinsic grain size effect. The above observation of X-ray diffraction and microstructure examination offers a plausible explanation on the phenomenon of dielectric properties of BCTZM ceramics which is closely related to the small change of the A/B ratio.

3.2.2 Breakdown voltage

As shown in Table I of the dielectric properties of BCTZM with small change of A/B ratio, most of the dielectric properties are proportional to grain size. Whereas, on the contrary, breakdown is approximately

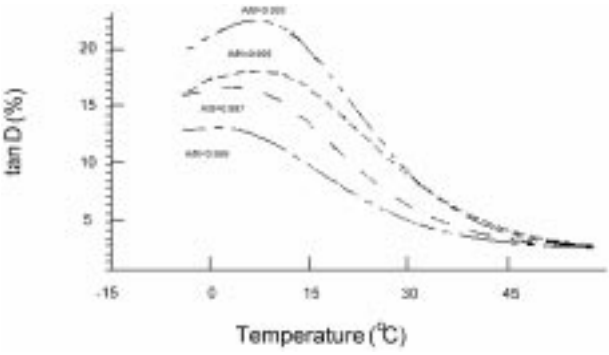

Figure 11 Temperature dependence of loss tangent for BCTZM samples with various A/B ratios.

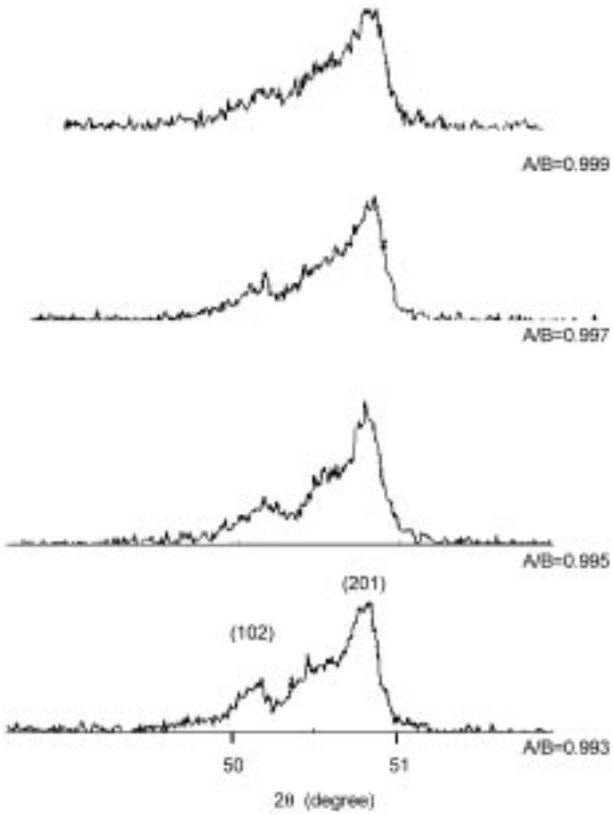

Figure 12 XRD patterns with step scan from 50° to 52° for BCTZM samples with various A/B ratios sintered at 1340 °C in 3% H_2/N_2 atmosphere and 25 °C H_2O.

inversely proportional to grain size. The breakdown is increased from 450 V to 550 V when the grain size is decreased from 8.1 μm to 4.9 μm. The breakdown at room temperature shows a progressive increase as grain size decreases. The increase in conductivity has been explained by the formation of oxygen vacancies and the accompanying reduction of titanium ions to the trivalent state [21].

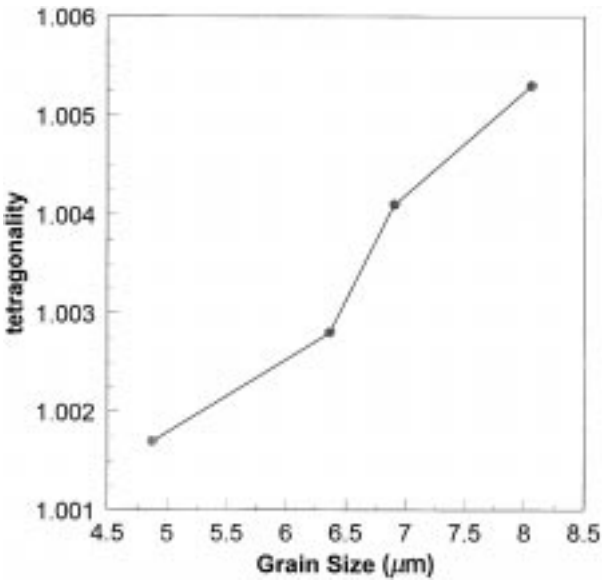

Figure 13 Grain size dependence of tetragonality.

TABLE I Variation of lattice parameter, grain size, loss tangent, Curie temperature and breakdown voltage of BCTZM sample with various A/B ratios

Ba/Ti	c/a	Grain size (μm)	K_{max}	tan$D$ 25 °C (%)	T_c (°C)	Breakdown voltage (V)
0.999	1.0017	4.88	11337	7.5	4	550
0.997	1.0028	6.37	12400	10	7	510
0.995	1.0041	6.91	13600	12.3	11	490
0.993	1.0053	8.06	15958	13.4	15	450

$$BaTi^{+4}O_3 \underset{\text{Reduction}}{\longrightarrow} BaTi^{+4}_{1-2x}Ti^{+3}_{2x}O_{3-x} + x/2\,O_2$$

Fig. 14 shows the breakdown of samples related to different grain size which were caused by the change of processing. Breakdown of BCTZM samples with different grain size attributed to sintering temperature and A/B ratio effect decreases with increasing grain size. On the other hand, it seems that there are no significant differences in breakdown of BCTZM with different grain size caused by the change of the sintering atmosphere.

The high breakdown of MLCC components is mainly caused by the fact that grain boundaries in the dielectric ceramic act as highly resistive barriers for cross transport of charge carriers. The conduction is of a mixed electronic-ionic nature because of holes h^o and oxygen vacancies V^{oo} as mobile carriers. Therefore, BCTZM with a small grain size was associated with more grain boundaries, per unit volume of the microstructure, which act as a barrier to prevent transport, in comparison to a large grain size. Presumably, high breakdown is often observed on BCTZM samples with small grain size by reducing the sintering temperature or increasing the A/B ratio. However, such a behavior of grain size dependence of breakdown seems to be invalid when the change of grain size was attributed to the various sintering atmospheres.

On the other hand, according to previous reports [22, 23] in the case of BCTZM sintered in a reducing atmosphere, the long lifetime sample which was sintered at a lower oxygen partial pressure, had a large grain size. The presence of grain boundary phase and grain boundary surface area per unit volume of the microstructure decreased as the grain size increased. The grain boundary phase formed due to the diffusion of Ni from the electrodes tended to occur mainly at higher oxygen partial pressures and it is presumably the cause of the deterioration of the characteristics of grain boundary and gives rise to a poor lifetime. Similarly, the effect of grain size on breakdown due to the change of sintering atmosphere in our study can be interpreted using the balance between the presence of the grain boundary phase and grain size effects. In other words, when sintering is at a lower oxygen partial pressure, the grain size is larger which is detrimental to breakdown voltage, and the amount of grain boundary phase is less, which is beneficial to breakdown voltage. In contrast, the grain boundary surface area per unit volume of the microstructure increased as the grain size decreased.

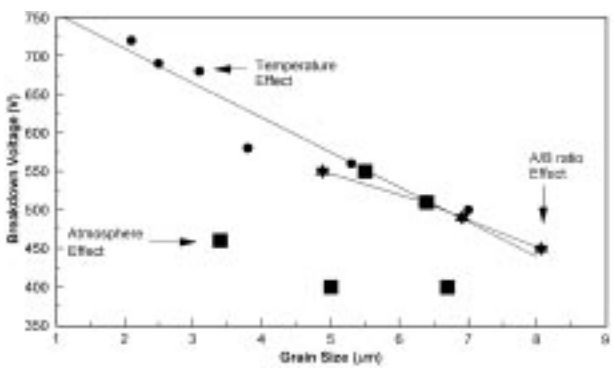

Figure 14 Breakdown voltage as a function of mean grain size for BCTZM samples.

4. Conclusion

1. Grain size is enhanced with increasing sintering temperature, decreasing A/B ratio and decreasing oxygen partial pressure for BCTZ + 1 mol % MnO_2 sintered in a reducing atmosphere. Concurrent with the grain size reduction, the crystal structure transformed from tetragonal to pseudocubic at room temperature and the dielectric constant, dissipation factor and Curie point are all decreased.

2. A marked influence of grain size on the performance of breakdown voltage is observed. Breakdown voltage is increased with decreasing grain size resulting from the sintering temperature and the A/B ratio and is approximately proportional to the reciprocal of the grain size which represents the number of grain boundaries as a barrier. However, there is no systematic tendency of breakdown when grain size is changed with oxygen partial pressure.

References

1. S. B. HERNER, F. A. SELMI, V. V. VARADAN and V. K. VARADAN, *Mater. Lett.* **15** (1993) 317.
2. I. BURN, 1976 Pacific Coast Regional Meeting of the American Ceramic Society, San Francisco, Calif., Nov. 2 (No. 99-BEN-76P).
3. H. SHIZUNO, S. KUSUMI, H. SAITO and H. KISHI, *Jpn. J. Appl. Phys.* **32** (1993) 4380.
4. T. K. GUPTA, *J. Mater. Res.* **7** (1992) 1023–28.
5. P. REN and S. ISHIDA, *J. Ceram. Soc. Jpn.* **103** (1995) 759.
6. J. M. HERBERT ''Ceramic Dielectric and Capacitor,'' Ch. 3 ''Method of Manufacture'', p. 84.
7. M. DEMARTIN, G. HERARD, C. CARRY and J. LEMAITRE, *J. Am. Ceram. Soc.* **80** (1997) 1079.
8. T. YAMAMOTO, *Brit. Ceram. Trans.* **94** (1995) 324.
9. J. S. CHOI and H. G. KIM, Proceedings of the 3rd International Conference on Properties and Application of Dielectric Materials, July 8–12 Tokyo, Japan, 1991.
10. D. T. D. HENNINGS, R. JANNSEN and P. J. L. REYNEN, *Brit. Ceram. Trans.* **70** (1987) 23.
11. M. DROFENIK, *J. Am. Ceram. Soc.* **70** (1987) 311.
12. Y. SAKABE, K. MINAI and K. WAKINO, *Jpn. J. Appl. Phys.* **20** (1981) 147.
13. R. WASER, *J. Am. Ceram. Soc.* **74** (1934) 40.

14. Y. NAKANO, A. SATOH, A. HITOMI and T. NOMURA, *Ceram. Trans*. pp 119.
15. T. R. ARMSTRONG, L. E. MORGENS, A. K. MAURICE and R. C. BUCHANAN, *J. Am. Ceram. Soc*. **72** (1989) 605.
16. G. ART, D. HENNINGS and G. DE WITH, *J. Appl. Phys*. **58** (1985) 15.
17. K. KINOSHITA and A. YAMAJI, *ibid*. **47** (1976).
18. K. KAGETAMA, *J. Am. Ceram. Soc*. **75** (1992) 1767.
19. D. HENNINGS and A. SCHNELL, *ibid*. **65** (1982) 539.
20. K. UCHION, E. SADANAGA, K. OONISHI and H. YAMAMURA, *Ceram. Trans*. **8** (1990) 107.
21. W. HEYWANG, *J. Mater. Sci*. **6** (1971) 1214.
22. Y. YONEDA, T. HOSOKAWA, N. OMORI, S. TAKEUCHI Carts-Europe'96: Tenth European Passive Components Symposium (1996) 11.
23. S. SUMITA, M. LKEDA, Y. NAKANO, K. NISHIYAMA and T. NOMURA, *J. Am. Ceram. Soc*. **74** (1991) 2739.

Received 22 May 2000
and accepted 6 January 2001